

DNA Clutch Probes for Circulating Tumor DNA Analysis

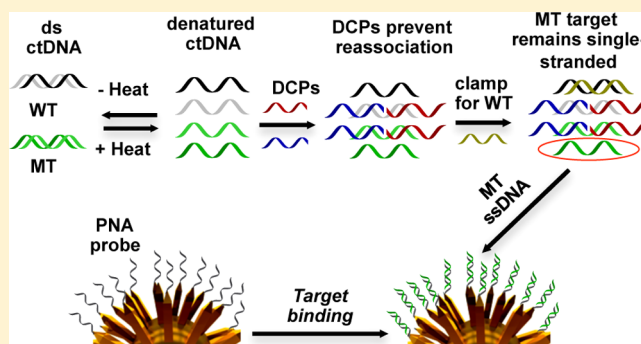
Jagotamoy Das,[†] Ivaylo Ivanov,[†] Edward H. Sargent,[‡] and Shana O. Kelley^{*,†,§}

[†]Department of Pharmaceutical Sciences, Leslie Dan Faculty of Pharmacy, and [‡]Department of Electrical and Computer Engineering, Faculty of Engineering, University of Toronto, Toronto, Ontario, Canada M5S 3M2

[§]Department of Biochemistry, Faculty of Medicine, University of Toronto, Toronto, Ontario, Canada M5S 3M2

S Supporting Information

ABSTRACT: Progress toward the development of minimally invasive liquid biopsies of disease is being bolstered by breakthroughs in the analysis of circulating tumor DNA (ctDNA): DNA released from cancer cells into the bloodstream. However, robust, sensitive, and specific methods of detecting this emerging analyte are lacking. ctDNA analysis has unique challenges, since it is imperative to distinguish circulating DNA from normal cells vs mutation-bearing sequences originating from tumors. Here we report the electrochemical detection of mutated ctDNA in samples collected from cancer patients. By developing a strategy relying on the use of DNA clutch probes (DCPs) that render specific sequences of ctDNA accessible, we were able to readout the presence of mutated ctDNA. DCPs prevent reassociation of denatured ctDNA. DCPs ensure thereby that only mutated sequences associate with chip-based sensors detecting hybridization events. The assay exhibits excellent sensitivity and specificity in the detection of mutated ctDNA: it detects 1 fg/μL of a target mutation in the presence of 100 pg/μL of wild-type DNA, corresponding to detecting mutations at a level of 0.01% relative to wild type. This approach allows accurate analysis of samples collected from lung cancer and melanoma patients. This work represents the first detection of ctDNA without enzymatic amplification.



INTRODUCTION

The analysis of circulating nucleic acids, such as cell-free tumor DNA and RNA, is poised to enable liquid biopsy approaches in cancer management. This type of minimally invasive assay stands to facilitate efficient diagnosis, prognostic analysis, and patient follow-up^{1–5} in comparison with tumor tissue biopsies that are notoriously painful, costly, and time-consuming. Circulating tumor DNA (ctDNA) is particularly informative as a molecular marker, since DNA is more chemically and biochemically stable than RNA.^{6,7}

Currently, there are few robust, sensitive, and specific detection methods for ctDNA analysis, and DNA sequencing is the only method that is effective.⁸ The double-stranded structure of DNA makes this molecular species a particularly challenging target for direct analysis. Biological interferences can limit the sensitivity of methods based on the polymerase chain reaction (PCR), and methods based on DNA hybridization allow high levels of sequence specificity, but are complicated by the reannealing of denatured single-stranded DNAs (ssDNAs), which hinders the hybridization between the denatured DNA and the probe.^{9–11} DNA sequencing has enabled important research studies, but the time frame associated with obtaining sequence information (2–3 weeks) does not address the needs of patients and physicians, and it is costly and provides unnecessarily detailed information.¹²

Patients affected with cancer can have higher levels of circulating DNAs than healthy individuals; however, the overall levels of circulating DNAs have significant variability in plasma or serum samples collected from each group.¹ For meaningful clinical analysis, specific cancer-related sequences must therefore be detected in ctDNA. Detection of tumor-specific mutations (e.g., *KRAS* and *BRAF*) in ctDNAs could facilitate specific monitoring of cancer-related sequences in the presence of normal DNA.^{13,14} However, detection of mutated ctDNAs is very challenging, because (i) denatured ctDNAs can reanneal without hybridizing to the probe, (ii) mutated ctDNAs are present at very low abundance, and (iii) low levels of mutant genes are present along with significant levels of normal DNA in patient samples. Therefore, for successful detection of mutated ctDNAs, a method should prevent reannealing of ssDNAs and must be highly sensitive and selective to detect low abundance mutated ctDNAs in the presence of a high background of unmutated sequences in patient samples.

Electronic and electrochemical chip-based methods offer attractive solutions for clinical sample analysis because they are straightforward to automate and implement using cost-effective instrumentation.^{15,16} Electrochemical detection methods are of

Received: June 9, 2016

Published: August 11, 2016

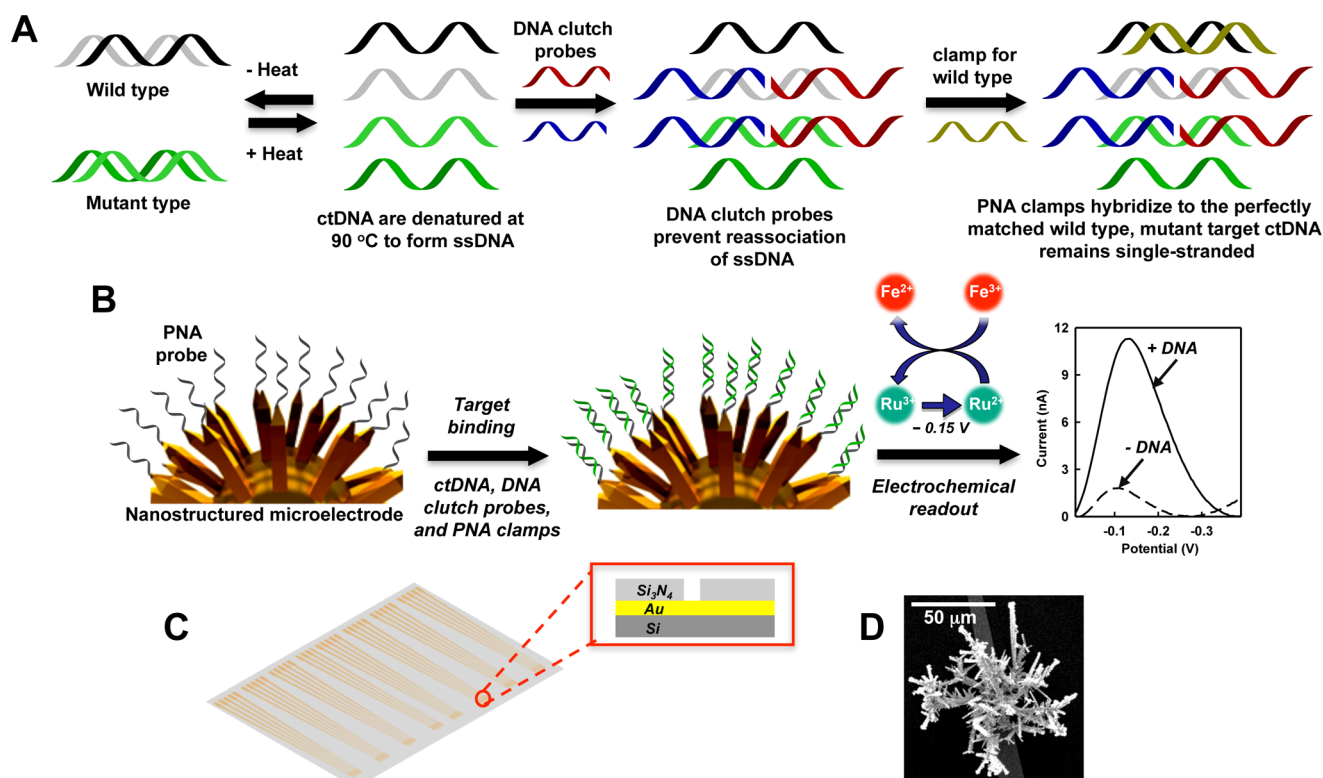


Figure 1. Schematic of clutch probe strategy for ctDNA detection. (A) *Detection strategy.* First, DNA double helices are denatured at 90 °C to form ssDNA. DNA clutch oligonucleotide probes are then used to prevent reassociation of ssDNA strands. The PNA clamps block wild-type target ssDNA and the mutant target ssDNA remains unhybridized. (B) *Chip-based detection.* NMEs are functionalized with PNA probes complementary to mutant target DNA. Only the complementary mutant targets bind to the probe. Finally, after hybridization of target sequences and washing, the signal generated from individual sensors was measured in the presence of an electrocatalytic reporter system using differential pulse voltammetry. (C) *Sensor chip layout.* Sensors were arrayed on a microchip where patterned apertures provide a template for the electrodeposition of gold. The inset shows cross-section of the chip at aperture. (D) An image of a nanostructured microelectrode sensor visualized using scanning electron microscopy.

particular interest because of their low cost, the high levels of multiplexing that can be achieved, and sensitivity.¹⁷ Electrochemical testing approaches have been applied successfully to analyze cancer biomarkers,^{18–24} as well as a variety of infectious pathogens,^{25–28} but have not been applied to ctDNA or mutated ctDNA analysis. The detection of point mutations based on electrochemical methods^{29–31} has been achieved, but the approaches used would not achieve a significant level of specificity in patient samples where mutated sequences may be present with a high background of the wild-type sequences and moreover, they are not capable of analyzing dsDNA. Alternatively, systems have been developed to analyze dsDNA directly, for example using DNA-binding zinc finger proteins,^{11,32–36} but these have been limited to proof-of-concept experiments. Overall, none of these methods analyze ctDNAs for cancer-related mutations in clinical samples.

Recently, we reported an electrochemical strategy that was the first to facilitate the direct interrogation of circulating tumor nucleic acids from patient serum samples.³⁷ Designer clamp molecules minimized cross-reactivity with wild-type nucleic acids and other mutational variants. The approach was highly specific, rapid, and sensitive to detect circulating nucleic acids in cancer patient samples. Although this approach was successful to detect tumor-specific circulating RNAs, the strategy could not detect ctDNAs, likely because of the inability to target double-stranded molecules.

Here we report an electrochemical approach that detects mutated ctDNAs in patient samples using DNA clutch probes (DCPs). DNA clutch probes are pairs of ssDNA molecules that prevent reassociation of denatured ssDNAs (Figure 1). As a result, they make one of the ssDNA strands from each dsDNA molecule available for hybridization to the probe. We functionalized nanostructured microelectrodes with PNA probes specific to a specific mutant DNA sequence, and a series of PNA clamps³⁷ were used to achieve high specificity so that the sensors could differentiate mutated DNA sequence from wild-type DNA sequence and other similar mutant sequence. We successfully detect mutated ctDNA in lung cancer and melanoma patient samples.

RESULTS AND DISCUSSION

Strategy for ctDNA Detection using DNA Clutch Probes. The design of the DCP electrochemical assay for analysis of mutated ctDNA is depicted in Figure 1. In real samples, target mutant ctDNAs are accompanied by large number of wild-type ctDNAs; however, for simplicity, we illustrate only two dsDNAs in Figure 1, one a wild-type dsDNA, and another mutant-type dsDNA. In a first phase, dsDNAs are denatured to form ssDNA by heating them to 90 °C. The DCPs are designed to hybridize to one of the ssDNA strands (they are complementary to that strand) and thereby they prevent reassociation of the DNA strands.

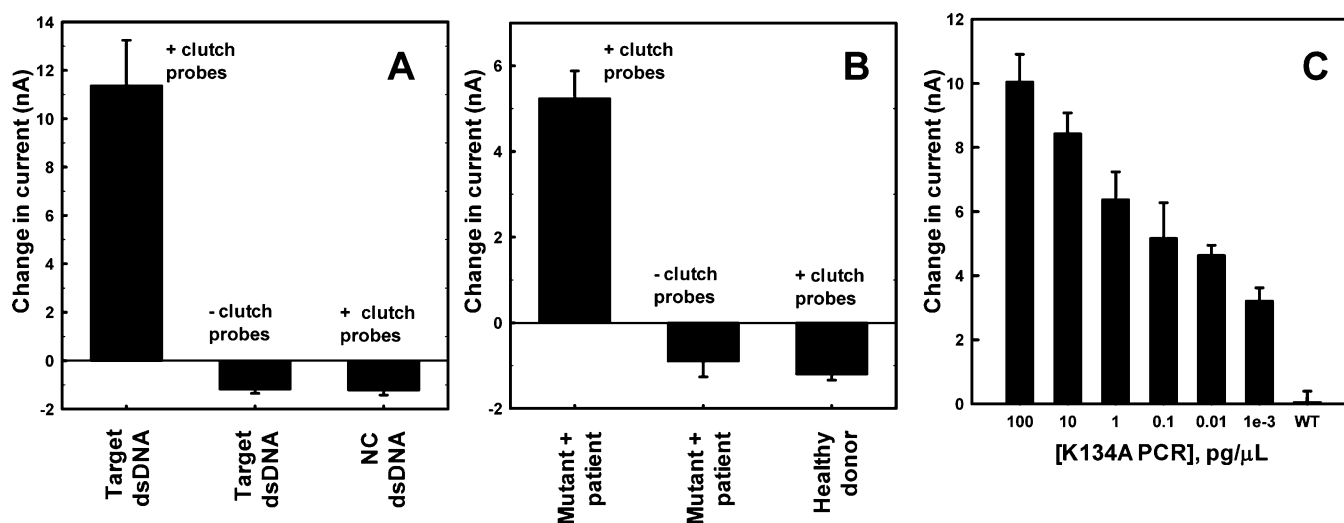


Figure 2. Sensitivity and specificity of the ctDNA assay. (A) Electrochemical signals observed in the absence and presence of DNA clutch probes (DCPs). Sensors functionalized with PNA probes corresponding to the *KRAS* 134A gene were challenged with mixtures of 134A PCR dsDNA (1 ng/μL) containing DCPs and PNA clamps, 134A PCR dsDNA (1 ng/μL) containing PNA clamps and but not DCPs, and noncomplementary (NC) PCR dsDNA (1 ng/μL) containing DCPs and PNA clamps. (B) Electrochemical signals observed with ctDNA isolated from a mutant-positive lung cancer patient sample in the absence and presence of DCPs. Sensors functionalized with universal *KRAS* PNA probes corresponding to the *KRAS* mutant gene were challenged with mixtures of ctDNA isolated from a mutant positive lung cancer patient sample containing DCPs and PNA clamp for wild-type gene, ctDNA isolated from the same mutant positive patient sample containing PNA clamp for wild-type gene and without DCPs, and ctDNA isolated from a healthy donor (HD) containing both DCPs and PNA clamp for wild type. (C) Concentration-dependent signal change for 134A PCR dsDNA in samples containing DCPs and clamp for WT, and 100 pg/μL WT PCR dsDNA at the 134A mutant sensor. WT represents wild-type target.

DNA Clutch Probe Design: Thermodynamic Considerations. Since the DCP is also complementary to the PNA probe immobilized to the NME sensor, we divide each DCP into two separate oligonucleotides. As a result, the stability of the target-probe complex is much higher than that between the DCPs and the PNA probe (i.e., the free energy (ΔG) is more negative, and the melting temperature is much higher). For example, the melting temperature of the PNA probe and one of the mutant target of *KRAS* gene (134A) complex is approximately 86 °C whereas melting temperatures of two of the DCPs and PNA probe complexes are 53 and 42 °C (Table S1 of the Supporting Information). In contrast, the free energy between the DCPs and one of the ssDNA is negative enough that the complex is stable at the hybridization temperature (melting temperatures are approximately 82 and 86 °C and free energy values are -51.6 kcal/mol and -54.9 kcal/mol) (Table S1).

Mutational Analysis Approach. To achieve the specific detection of mutated ctDNA, we use PNA clamps: these hybridize to the wild-type ssDNA, preventing hybridization with the probe. To prevent binding of sequences that do not contain the mutation of interest, we designed the clamps so that they would target each of the mutants (except the detection target) as well as the wild-type sequence. We then introduce this mixture of clamps onto a sensor chip that has been functionalized with a PNA probe corresponding to the mutant gene. Only the targeted mutant hybridizes to the probe; all other mutations and the wild-type sequence are blocked by their clamps and simply remain in solution and are washed away (Figure 1B). After 30 min, we measure the electrochemical signal and determine the identity of the sequence.

We chose the *KRAS* gene as one target for initial testing; this sequence has 7 somatic mutations at codons 12 and 13 of exon 2, which are 135A, 135C, 135T, 134A, 134C, 134T, and 138A.

We also selected the *BRAF* gene, which has a mutation at 1799 $T > A$, as a model detection targets. Mutated *KRAS* (Kirsten rat sarcoma-2 virus) genes are associated with different cancers, including lung cancer, colorectal cancer, and ovarian cancer,^{2,5,14,38,39} and the effectiveness of targeted therapies are affected by the mutations. The mutated *BRAF* gene is associated with a dangerous skin cancer, melanoma.

Electrochemical Sensors and Redox Readout System. Photolithographic patterning was used to produce an array of 40 sensors for multiplexed ctDNA analysis (Figure 1C). A SiO_2 -coated silicon wafer was used as a substrate for the patterning of gold contact pads and electrical leads. On top of the gold pattern, a layer of Si_3N_4 was deposited to form an insulating layer on the top surface of the integrated circuit. A templated surface for the growth of electrodeposited sensors was formed by using photolithography to create 5 μm openings in the Si_3N_4 insulating layer. We electrodeposited gold in the patterned apertures to deposit three-dimensional microsensors. The three-dimensional sensors extend from the chip surface into solution,^{20,27,40,41} and have sizes and morphologies that can be manipulated with deposition time, deposition potential, gold ion concentration, and electrolyte composition. Since nanostructuring enhances the sensitivity of the assay,^{27,42–45} we electrodeposited the Au structures with a fine layer of Pd to produce nanostructured microelectrodes (NMEs). A SEM image of a NME is shown in Figure 1D. The micron-size scale of the three-dimensional electrodes increases the surface area available for interaction with analyte molecules, while the nanostructuring enhances the hybridization efficiency between tethered probes and analytes in solution.⁴⁶

We immobilized PNA probes complementary to mutated sequences on the NMEs (Figure 1B). Following target hybridization and washing, we used an electrocatalytic redox couple composed of $\text{Ru}(\text{NH}_3)_6^{3+}$ and $\text{Fe}(\text{CN})_6^{3-}$ to detect the

presence of specific ctDNA sequences.⁴⁷ $\text{Ru}(\text{NH}_3)_6^{3+}$ is accumulated at the electrode surface via electrostatic attraction to the negatively charged DNAs that bind to the sensor surface and is converted to $\text{Ru}(\text{NH}_3)_6^{2+}$ when the electrode reaches the reduction potential. $\text{Ru}(\text{NH}_3)_6^{2+}$ is chemically oxidized back to $\text{Ru}(\text{NH}_3)_6^{3+}$ by the $\text{Fe}(\text{CN})_6^{3-}$ present in solution allowing for multiple turnovers of $\text{Ru}(\text{NH}_3)_6^{3+}$, and significant signal amplification. The increase of the posthybridization current relative to the prehybridization current is used as a measure to determine target hybridization (typical differential pulse voltammograms (DPVs) before and after incubation with a solution containing 1 ng/ μL PCR products (134A) is shown in Figure 1B).

Sensitivity and Specificity Studies with PCR Products.

The arrayed sensor chip was designed to interrogate samples to probe for the presence of seven individual lung-cancer associated point mutations of the *KRAS* gene. A set of DCPs, PNA probes, and PNA clamps was designed, synthesized, and tested to determine whether the electrochemical approach could produce comparable results to existing PCR-based methods.

To validate the detection principle, we challenged sensors modified with one of the PNA probes specific to the mutant target (for instance, here we use PNA probe specific to the 134A mutant gene) with PCR products mixed with DCPs and PNA clamps; PCR products mixed with PNA clamps but without DCPs; and noncomplementary PCR dsDNA with DCPs and PNA clamps. We only observed signal changes with complementary PCR dsDNA in the presence of DCPs (Figure 2A). No signal change in absence of DCPs indicates inefficient hybridization of DNA, due to reassociation of the DNA strands. These results clearly illustrate that DCPs are necessary for detection of dsDNA.

After confirming that DCPs are necessary for detection of PCR dsDNA, we investigated if DCPs are necessary to detect mutated ctDNA. We challenged sensors modified with a universal PNA probe³⁷ mixture specific to all of the possible types of mutations in *KRAS* gene with ctDNA isolated from a mutant positive lung cancer patient mixed with DCPs and PNA clamps; ctDNA isolated from same patient sample mixed with PNA clamps but without DCPs; and ctDNA isolated from a healthy control with DCPs and PNA clamps. We only observed signal changes with ctDNA isolated from a mutant positive patient in the presence of DCPs (Figure 2B). No signal change in absence of DCPs indicates inefficient hybridization of mutated ctDNA. Further, no signal change with ctDNA isolated from a healthy control indicate that our sensor is very specific. These results clearly illustrate that DCPs are necessary for detection of ctDNA and our previously developed electrochemical clamp assay is unsuccessful to detect ctDNA. The percentage of mutation in this sample was approximately 1.6% calculated by clamp PCR.

We investigated the sensitivity of the ctDNA assay by monitoring the dependence of the electrochemical signal on the concentration of PCR products containing the 134A mutation. Wild-type PCR products were used to evaluate specificity. Concentration-dependent titration data (Figure 2C) were obtained with variable concentration of 134A PCR products in the presence of 10 nM of each of the DNA clutch probes, 10 nM PNA clamps for WT, and 100 pg/ μL WT PCR products. To determine the detection limit of the DCP assay, we analyzed solutions containing PCR products at concentrations ranging from 1 fg/ μL to 100 pg/ μL (Figure 2C). The signals

increased with increasing concentration of the target over this range. It is apparent from the results that our sensor can detect 1 fg/ μL target mutation in the presence of 100 pg/ μL of wild-type PCR products, which means that our sensor is able to detect 0.01% mutations. This level of sensitivity is similar to that achieved with a similar assay for cell-free RNA.³⁷

A high level of specificity is achieved here using PNA clamps. A high level of sensitivity is obtained by using NMEs coupled with an electrocatalytic reporter system to detect low levels of mutations. NMEs improve hybridization efficiency due to their three-dimensional structures that feature large surface areas along with nanostructured surfaces. While the 3D structure increases the probability of interactions with target molecules, the nanostructured surfaces display probes in an active orientation that promotes accessibility and binding of targeted sequences. Moreover, the electrocatalytic reporter system amplifies the signal significantly (more than 30-fold) by regenerating the redox reporter probes.

Discrimination of Homozygous and Heterozygous Mutants. Given the importance of distinguishing homozygous from heterozygous mutants,⁴⁸ we investigated whether the new assay was sufficiently specific to discriminate among the different mutant profiles. Sensors were functionalized simultaneously using eight different probes of *KRAS* gene (seven mutant probes and one wild-type probe) (Figure 3A) and were

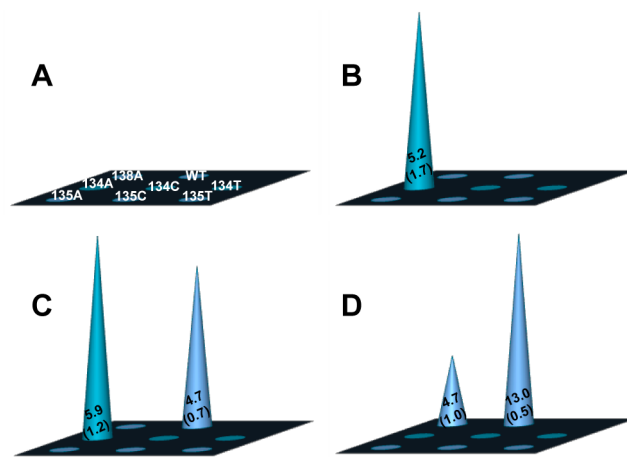


Figure 3. Detection of samples corresponding to homozygous and heterozygous *KRAS* mutants. (A) Chip layout for array enabling detection of seven mutant alleles of *KRAS* and wild type. (B) Response of mutant array chip challenged with 1 nM of 134A target DNA (19 bp) (C) Response of chip challenged with equimolar mixture (1 nM of each) of 134A and wild-type target DNA. (D) Response of chip challenged with ctDNAs isolated from a mutant-positive lung cancer patient.

challenged with DNAs and a mutant positive patient sample. Sensors were first challenged with 1 nM synthetic target (19 bp length) containing the 134A mutation (Figure 3B). The response of sensors modified with the 134A mutant probe was significant, whereas no other probes showed significant response to this target. We also challenged the sensors with a mixture of 134A mutant target and wild-type target (Figure 3C). The response of sensors modified with the 134A mutant probe and wild type was significant, whereas none of the other probes showed an appreciable response to this DNA mixture. In addition, to examine the ability of our sensors to detect ctDNA mutations, we challenged our sensors with mutant-

positive lung cancer patient samples. Only electrodes functionalized with the 138A probe and wild-type probe showed a significant electrochemical response. These results indicate that this patient sample has the 138A mutation in addition to the wild-type sequence. The percentage of mutation in the ctDNA was found approximately 0.1% (calculated using clamp PCR). These results illustrate that the multiplexing provided by chip enables the parallelized detection of ctDNA mutations and ability to discriminate targets with very similar sequences. These results further illustrate that our chip can identify any of the known mutations at codons 12 and 13 of exon 2 of *KRAS* gene specifically. Moreover, using a universal probe mixture we are able to know any possible type of mutations at those positions *KRAS* gene.

Analysis of ctDNA in Lung and Melanoma Patient Samples. The ultimate goal for the DCP assay was to prove that it was effective in detecting mutated ctDNAs in patient samples. We tested the ability of the electrochemical assay to produce results comparable to a PCR-based method by analyzing ctDNA in serum collected from lung cancer patients (*KRAS* mutations) and melanoma patients (*BRAF* mutations) (Tables 1 and 2). In the studies monitoring *KRAS*, a universal probe mixture³⁷ was used that permitted parallel analysis for all possible known mutations in ctDNAs.

Table 1. Detection of Mutated ctDNA in Samples Collected from Lung Cancer Patients^a

sample	DCP chip analysis		clamp PCR analysis		
	ΔI (nA)	assessment	$\Delta Ct-1$	$\Delta Ct-2$	assessment
1	-1.4 ± 0.2	wild type			wild type
2	6.0 ± 0.5	KRAS mutated	6	7	KRAS mutated
3	-0.9 ± 0.4	wild type			wild type
4	-1.4 ± 0.3	wild type	-2	16	wild type
5	12.5 ± 1.3	KRAS mutated	3	6	KRAS mutated
6	-0.7 ± 0.2	wild type			wild type
7	8.6 ± 1.0	KRAS mutated	4	6	KRAS mutated
8	-1.0 ± 0.2	wild type	-1	14	wild type
9	-1.2 ± 0.4	wild type	-3	14	wild type
HD1	0.2 ± 0.4	wild type			wild type
HD2	-0.7 ± 0.1	wild type	-3	10	wild type

^aDCP chip-based sensors were challenged with circulating DNAs from lung cancer patients. For the DCP chip-based analysis of ctDNAs, the cutoff threshold for the sensors was 1.65 nA. ^bFor clamp PCR, values $\Delta Ct-1 \geq 2$ are indicative of mutated sequences and $\Delta Ct-1$ values < 0 are indicative of wild-type sequences. If $0 < \Delta Ct-1 < 2$, then $\Delta Ct-2$ should be analyzed and if $\Delta Ct-2 > 6$, then the sample is considered to be wild-type. Error values are standard errors. The cycle number where a detectable signal is generated is referred to as the cycle threshold (Ct). $\Delta Ct-1$ values are calculated using the expression: $\Delta Ct-1 = (\text{Standard Ct}) - (\text{Sample Ct})$ and $\Delta Ct-2$ values are derived by analyzing Ct values of the non PNA mix versus the Ct values of the samples, e.g., $\Delta Ct-2 = (\text{Sample Ct}) - (\text{non PNA mix Ct})$. The standard Ct is 35 for the 7500 AB thermocycler used for this experiment.

Serum samples collected from 9 lung cancer and 9 melanoma patients were analyzed for ctDNA mutations, along with samples collected from healthy individuals. For the lung cancer patients, three of the nine lung cancer patient samples were positive for *KRAS* mutations, and three of the nine melanoma patient samples were positive for *BRAF* mutations. A cutoff value was calculated from the mean signal collected from a healthy donor sample plus three standard deviations. If the

Table 2. Detection of Mutated ctDNA in Samples Collected from Melanoma Patients^a

sample	DCP chip analysis		clamp PCR analysis		
	ΔI (nA)	assessment	$\Delta Ct-1$	$\Delta Ct-2$	assessment
1	-0.5 ± 0.3	wild type	0	11	wild type
2	-1.1 ± 0.5	wild type	0	12	wild type
3	-1.3 ± 0.4	wild type	-1	11	wild type
4	7.9 ± 1.0	BRAF mutated	3	7	BRAF mutated
5	0.3 ± 0.3	wild type	1	10	wild type
6	-1.3 ± 0.5	wild type	1	11	wild type
7	7.1 ± 1.0	BRAF mutated	1	11	wild type
8	8.4 ± 0.7	BRAF mutated	3	8	BRAF mutated
9	-0.3 ± 0.6	wild type	1	13	wild type
HD	-2 ± 0.1	wild type	-2	12	wild type

^aSee Table 1 for details of analysis.

signal collected from a patient sample was higher than the cutoff value, then the sample was called positive for the mutation, and if it is lower, then the sample was negative for the mutation. For each sample, a clamp PCR⁴⁹ method was also used to test for *KRAS* and *BRAF* mutations, and the results obtained using this approach agreed with the results obtained using the DCP electrochemical assay.

It is noteworthy that although the PCR signal was undetermined in case of melanoma sample 7, the new assay reported herein was successful in detecting mutation in this sample. The abundance of mutations found (using clamp PCR) in lung cancer patient samples of sample 2, sample 5, and sample 7 were approximately 0.7%, 1.6%, and 1.6%, respectively (Table 1) and 0.8% and 0.1% mutation were found in sample 4 and sample 8 respectively of melanoma patients (Table 2).

Conventional PCR methods, including real-time PCR, cannot detect mutated ctDNA as they cannot detect minor variants at levels $< 20\%$. COLD-PCR (coamplification at lower denaturation temperature-PCR) is a good strategy for mutation detection, as it is able to detect mutations down to 0.5–1%.⁵⁰ However, COLD-PCR requires critical control of the denaturation temperatures, necessitating a thermocycler with a high degree of accuracy. Moreover, COLD-PCR is typically coupled with DNA sequencing for confirmation of the abundance of mutant sequences. Digital PCR is another good method for the detection of mutations in ctDNA. For example droplet digital PCR is enabled to detect mutation down to 0.1 to 0.05%.⁵¹ But use of digital PCR is limited due its high cost.⁵² Moreover, the sensitivity of PCR methods is often reduced because of interference from chemical species present in clinical samples. In contrast, our method can detect mutation down to 0.01%, which is comparable to digital PCR.

CONCLUSIONS

We have analyzed the ctDNA contained in samples collected from lung cancer and melanoma patients using an electrochemical assay exhibiting high levels of sensitivity and specificity. The specificity of our method approaches 0.01%. The results match what can be obtained with standard PCR-based methods. The clamp chip that we developed previously successfully detected mutated circulating RNA accurately but could not detect ctDNA. The DCP approach that we introduce in the present work prevents the reassociation of ssDNAs, promoting hybridization to a PNA probe immobilized to the sensor. DCPs were designed such that the free energy (ΔG) between the target and the PNA probe was much lower (more

negative) than binding energy between the DCPs and the PNA probe. The collection of clamp sequences therefore compete with the target sequence and only allow the specific mutated target to bind to the chip. Minimally invasive analyses of ctDNA offer an attractive alternative to cancer tissue biopsies and offer a new means to monitor drug response and treatment efficacy. The sensitivity of our assay is extremely high, which facilitates the direct sampling of serum (rather than invasive sampling of a tumor) to profile the mutational spectrum of a tumor. The time required to analyze samples can be as short as 30 min, which is an advantage relative to the 2–3 h required for PCR. Finally, the use of a chip-based format for the assay lends itself to automation and incorporation of this type of testing into user-friendly instrumentation. Moreover, our assay could be expanded to monitor diseases caused by DNA viruses that have DNA as their genetic material.

MATERIALS AND METHODS

HAuCl₄ solution, potassium ferricyanide (K₃[Fe(CN)₆]), and hexamine ruthenium(III) chloride (Ru(NH₃)₆Cl₃) were obtained from Sigma-Aldrich. ACS-grade acetone, isopropyl alcohol (IPA), and perchloric acid were obtained from EMD; hydrochloric acid was purchased from VWR. Phosphate-buffered saline (PBS, pH 7.4, 1×) was obtained from Invitrogen. All of the PNA probes and PNA clamps were obtained from PNA Bio, U.S.A. PCR primers, synthetic DNA targets, and DNA clutch probes (DCPs) were obtained from ACGT, Canada. Lung cancer and melanoma patient serums were obtained from Bioreclamation Inc., U.S.A. PCR primers for BRAF (95bp PCR product): Forward primer: FPBRAF3 (5'-CCTCACAGTAAAAA-TAGGTGATTTTGG-3'), Reverse primer: RPBRAF3 (5'-CA-CAAAATGGATCCAGACAAGTTC-3'). PCR primers for KRAS (80bp PCR product): Forward primer: FPKRAS (5'-GCC-TGC-TGA-AAA-TGA-CTG-AAT-ATA-3'), Reverse primer: RPKRAS (5'-TTA-GCT-GTA-TCG-TCA-AGG-CAC-TC-3'). Sequences related to KRAS mutation detection: PNA probes for 135A, 135C, 135T, 134A, 134C, 134T, 138A, and Universal probe are Cys-Gly-CTA CGC CAG CAG CTC CAA C, Cys-Gly-CTA CGC CAG CAG CTC CAA C, Cys-Gly-CTA CGC CAA CAG CTC CAA C, Cys-Gly-CTA CGC CAC TAG CTC CAA C, Cys-Gly-CTA CGC CAG CTC CAA C, Cys-Gly-CTA CGC CAG CTC CAA C, Cys-Gly-CTA CGC CAG CTC CAA C, Cys-Gly-CTA CGT CAC CAG CTC CAA C, Cys-Gly-CTA CGX CAX XAG CTC CAA C (Where, X = mixture of A, T, and G with unimolar ratio) respectively. PNA clamps for 135A, 135C, 135T, 134A, 134C, 134T, 138A, WT (135G) are ACG CCA TCA GCT C, ACG CCA GCA GCT C, ACG CCA ACA GCT C, ACG CCA CTA GCT C, ACG CCA CGA GCT C, ACG CCA CAA GCT C, CCT ACG TCA CCA G, ACG CCA CCA GCT C, respectively. Synthetic ssDNA targets for 135A, 135C, 135T, 134A, 134C, 134T, 138A, WT (135G) are GTT GGA GCT GAT GGC GTA G, GTT GGA GCT GCT GGC GTA G, GTT GGA GCT GTT GGC GTA G, GTT GGA GCT AGT GGC GTA G, GTT GGA GCT CGT GGC GTA G, GTT GGA GCT TGT GGC GTA G, GTT GGA GCT GGT GAC GTA G, GTT GGA GCT GGT GGC GTA G respectively. DNA clutch probe 5' and DNA clutch probe 3' are CTG AAA ATG ACT GAA TAT AAA CTT GTG GTA GTT GGA GCT XX (where X = A, C, G, T is equimolar concentration) and TGX CGT AGG CAA GAG TGC CTT GAC GAT ACA GCT AAT TC respectively. Sequences related to BRAF mutation detection: Probe for BRAF mutant (1799 T > A) is Cys-Gly-GAT TTC TCT GTA GCT A. PNA clamp for BRAF WT is GAT TTC ACT GTA G. Synthetic ssDNA Target for BRAF mutant and WT are TAG CTA CAG AGA AAT C and TAG CTA CAG TGA AAT C respectively. DNA clutch probe 5' and DNA clutch probe 3' are GAA GAC TC ACA GTA AAA ATA GGT GAT TTT GGT CTA GCT ACA GA and GAA ATC TCG ATG GAG TGG GTC CCA TCA GTT TGA AC respectively.

Fabrication of NMEs. Chips were cleaned by sonication in acetone for 5 min, rinsed with isopropyl alcohol, and DI water, and dried with a flow of nitrogen. Electrodeposition was performed at

room temperature; 5 μm apertures on the fabricated electrodes were used as the working electrode and were contacted using the exposed bond pads. Au sensors were made using a deposition solution containing 50 mM solution of HAuCl₄ and 0.5 M HCl using DC potential amperometry at 0 mV for 100 s. After being washed with deionized water and drying, the Au sensors were coated with a thin layer of Pd to form nanostructures by replating in a solution of 5 mM H₂PdCl₄ and 0.5 M HClO₄ at -250 mV for 10 s. The control of sensor surface area has been characterized extensively⁵³ and in this study, the average surface area was 4.75 ± 0.3 × 10⁻⁴ cm² as determined by electrochemical Pd oxide stripping.

Sensor Preparation and Assay Protocol. Sensors were prepared and assays conducted as described previously.³⁷ The probe deposition conditions used here were shown previously to lead to a surface coverage of 2 × 10¹³ molecules/cm².⁴³ After the initial electrochemical scanning, the chips were treated with different targets at 65 °C for 30 min. This time point was selected based on prior work with RNA targets.³⁷ After being washed with PBS at 60 °C for 10 min followed by washing for 10 min at room temperature, an electrochemical scan of the chip was performed to assess sample hybridization.

ctDNA Isolation from Sera. Nucleic acids were isolated from patient sera using a Norgen Biotek kit catalogue number 51000. After isolation of bulk nucleic acids, we treated them with RNase A (Qiagen, 100 mg/mL) for 20 min at 37 °C to digest RNA (2 μL of RNase A was mixed with 6 μL of sample).

Sample Preparation. DNA samples were mixed with 100 nM PNA clamps, 100 nM DNA clutch probe 5', and 100 nM DNA clutch probe 3', and the mixture was heated at 90 °C for 2 min. After that the solution was chilled on ice for 2 min before being pipetted onto the sensors. For patient samples, we treated samples with RNase A (Qiagen, 100 mg/mL) to digest RNA.

ctDNA Synthesis and Clamp PCR. Purified nucleic acids (30–754 ng) dissolved in 2 μL was used for cDNA synthesis in 20 μL reactions with random hexamer primers and Superscript III reverse transcriptase. Two μL of cDNA was used in 50 μL not-competitive clamp PCR reaction with 2 μM final concentration of gene specific primers, and 100 nM of PNA clamps, or in a 20 μL of real-time clamp PCR reaction, Panagene kit. The clamp PCR was optimized as described previously.³⁷

Preparation of PCR Targets. Total RNA was isolated from cultured cells (cell lines A549, U373vIII, and WM9 have 134 A KRAS, wild-type KRAS and BRAF, and BRAF mutant (1799 T > A) genes, respectively) by Trizol reagent (Invitrogen) and used for RT-PCR as described previously.³⁹ The PCR products were purified by agarose gel electrophoresis and a gel extraction kit (Promega). The purified PCR products were diluted with water to a final concentration of 100 ng/μL.

Electrochemical Analysis. All electrochemical experiments were carried out using a Bioanalytical Systems Epsilon potentiostat with a three-electrode system featuring a Ag/AgCl reference electrode and a platinum wire auxiliary electrode. Electrochemical signals were measured in a 0.1 × PBS containing 10 μM [Ru(NH₃)₆]Cl₃, and 4 mM K₃[Fe(CN)₆]. Differential pulse voltammetry (DPV) signals were obtained with a potential step of 5 mV, pulse amplitude of 50 mV, pulse width 50 ms, and a pulse period of 100 ms. Signal changes corresponding to specific target were calculated with background-subtracted currents: change in currents = (I_{after} - I_{before}) (where I_{after} = current after target binding, I_{before} = current before target binding).

ASSOCIATED CONTENT

Supporting Information

The Supporting Information is available free of charge on the ACS Publications website at DOI: 10.1021/jacs.6b05679.

Concentration dependence of electrochemical DCP assay, Au plating curves, comparison of different sensors at same and different chips, and melting temperature of different duplexes (PDF)

■ AUTHOR INFORMATION

Corresponding Author

*shana.kelley@utoronto.ca

Author Contributions

The manuscript was written through contributions of all authors. All authors have given approval to the final version of the manuscript.

Notes

The authors declare no competing financial interest.

■ ACKNOWLEDGMENTS

This research was sponsored by the Ontario Research Fund (Research Excellence Award to S.O.K.), the Canadian Institutes for Health Research (Emerging Team Grant to S.O.K. and E.H.S.), the Canadian Cancer Society Research Institute (Innovation Grant #702414 to S.O.K.) and the Natural Science and Engineering Research Council (Discovery Grant to S.O.K.).

■ REFERENCES

(1) Schwarzenbach, H.; Hoon, D. S. B.; Pantel, K. *Nat. Rev. Cancer* **2011**, *11*, 426–437.

(2) Newman, A. M.; Bratman, S. V.; To, J.; Wynne, J. F.; Eclow, N. C. W.; Modlin, L. A.; Liu, C. L.; Neal, J. W.; Wakelee, H. A.; Merritt, R. E.; Shrager, J. B.; Loo, B. W., Jr.; Alizadeh, A. A.; Diehn, M. *Nat. Med.* **2014**, *20*, 548–556.

(3) García-Olmo, D. C.; Domínguez, C.; García-Arranz, M.; Anker, P.; Stroun, M.; García-Verdugo, J. M.; García-Olmo, D. *Cancer Res.* **2010**, *70*, 560–567.

(4) Bedard, P. L.; Hansen, A. R.; Ratain, M. J.; Siu, L. L. *Nature* **2013**, *501*, 355–364.

(5) Bettgowda, C.; Sausen, M.; Leary, R. J.; Kinde, I.; Wang, Y.; Agrawal, N.; Bartlett, B. R.; Wang, H.; Lubner, B.; Alani, R. M.; Antonarakis, E. S.; Azad, N. S.; Bardelli, A.; Brem, H.; Cameron, J. L.; Lee, C. C.; Fecher, L. A.; Gallia, G. L.; Gibbs, P.; Le, D.; Giuntoli, R. L.; Goggins, M.; Hogarty, M. D.; Holdhoff, M.; Hong, S.-M.; Jiao, Y.; Juhl, H. H.; Kim, J. J.; Siravegna, G.; Laheru, D. A.; Lauricella, C.; Lim, M.; Lipson, E. J.; Marie, S. K. N.; Netto, G. J.; Oliner, K. S.; Olivi, A.; Olsson, L.; Riggins, G. J.; Sartore-Bianchi, A.; Schmidt, K.; Shih, I.-M.; Oba-Shinjo, S. M.; Siena, S.; Theodorescu, D.; Tie, J.; Harkins, T. T.; Veronese, S.; Wang, T.-L.; Weingart, J. D.; Wolfgang, C. L.; Wood, L. D.; Xing, D.; Hruban, R. H.; Wu, J.; Allen, P. J.; Schmidt, C. M.; Choti, M. A.; Velculescu, V. E.; Kinzler, K. W.; Vogelstein, B.; Papadopoulos, N.; Diaz, L. A. *Sci. Transl. Med.* **2014**, *6*, 224ra24.

(6) Silverman, S. K. *Acc. Chem. Res.* **2009**, *42*, 1521–1531.

(7) Stutterheim, J.; Ichou, F. A.; Ouden, E. d.; Versteeg, R.; Caron, H. N.; Tytgat, G. A. M.; Schoot, C. E. v. d. *Clin. Cancer Res.* **2012**, *18*, 808–814.

(8) Junga, A. K.; Fleischhacker, M.; Rabierna, A. *Clin. Chim. Acta* **2010**, *411*, 1611–1624.

(9) Wang, X.; Lim, H. J.; Son, A. *Environ. Health Toxicol.* **2014**, *29*, e2014007.

(10) Raap, A. K.; Marijnen, J. G. J.; Vrolijk, J.; Ploeg, M. v. d. *Cytometry* **1986**, *7*, 235–242.

(11) Noh, S.; Ha, D. T.; Yang, H.; Kim, M.-S. *Analyst* **2015**, *140*, 3947–3952.

(12) Dewey, F. E.; Pan, S.; Wheeler, M. T.; Quake, S. R.; Ashley, E. A. *Circulation* **2012**, *125*, 931–944.

(13) Thierry, A. R.; Mouliere, F.; El Messaoudi, S.; Mollevi, C.; Lopez-Crapez, E.; Rolet, F.; Gillet, B.; Gongora, C.; Dechelotte, P.; Robert, B.; Del Rio, M.; Lamy, P.-J.; Bibeau, F.; Nouaille, M.; Lorient, V.; Jarrousse, A.-S.; Molina, F.; MATHONNET, M.; Pezet, D.; Ychou, M. *Nat. Med.* **2014**, *20*, 430–436.

(14) Huber, F.; Lang, H. P.; Backmann, N.; Rimoldi, D.; Gerber, C. *Nat. Nanotechnol.* **2013**, *8*, 125–129.

(15) Kelley, S. O.; Mirkin, C. A.; Walt, D. R.; Ismagilov, R. F.; Toner, M.; Sargent, E. H. *Nat. Nanotechnol.* **2014**, *9*, 969–980.

(16) Macazo, F. C.; White, R. J. *J. Am. Chem. Soc.* **2016**, *138*, 2793–2801.

(17) Bakker, E.; Qin, Y. *Anal. Chem.* **2006**, *78*, 3965–3983.

(18) Das, J.; Kelley, S. O. *Anal. Chem.* **2011**, *83*, 1167–1172.

(19) Wen, Y.; Pei, H.; Shen, Y.; Xi, J.; Lin, M.; Lu, N.; Shen, X.; Li, J.; Fan, C. *Sci. Rep.* **2012**, *2*, art. no. 867.

(20) Chuah, K.; Lai, L. M. H.; Goon, I. Y.; Parker, S. G.; Amal, R.; Gooding, J. J. *Chem. Commun.* **2012**, *48*, 3503–3505.

(21) Si, Y.; Sun, Z.; Zhang, N.; Qi, W.; Li, S.; Chen, L.; Wang, H. *Anal. Chem.* **2014**, *86*, 10406–10414.

(22) Rusling, J. F. *Anal. Chem.* **2013**, *85*, 5304–5310.

(23) Das, J.; Aziz, M. A.; Yang, H. *J. Am. Chem. Soc.* **2006**, *128*, 16022–16023.

(24) Mahshid, S. S.; Camire, S.; Ricci, F.; Vallee-Belisle, A. *J. Am. Chem. Soc.* **2015**, *137*, 15596–15599.

(25) Fang, Z.; Soleymani, L.; Pampalakis, G.; Yoshimoto, M.; Squire, J. A.; Sargent, E. H.; Kelley, S. O. *ACS Nano* **2009**, *3*, 3207–3213.

(26) Soleymani, L.; Fang, Z.; Lam, B.; Bin, X.; Vasilyeva, E.; Ross, A.; Sargent, E. H.; Kelley, S. O. *ACS Nano* **2011**, *5*, 3360–3366.

(27) Ferguson, B. S.; Buchsbaum, S. F.; Wu, T.-T.; Hsieh, K.; Xiao, Y.; Sun, R.; Soh, H. T. *J. Am. Chem. Soc.* **2011**, *133*, 9129–9135.

(28) Hsieh, K.; Patterson, A. S.; Ferguson, B. S.; Plaxco, K. W.; Soh, H. T. *Angew. Chem., Int. Ed.* **2012**, *51*, 4896–4900.

(29) Yang, H.; Hui, A.; Pampalakis, G.; Soleymani, L.; Liu, F.-F.; Sargent, E. H.; Kelley, S. O. *Angew. Chem., Int. Ed.* **2009**, *48*, 8461–8464.

(30) Wu, Y.; Lai, R. Y. *Chem. Commun.* **2013**, *49*, 3422–3424.

(31) McWilliams, M. A.; Bhui, R.; Taylor, D. W.; Slinker, J. D. *J. Am. Chem. Soc.* **2015**, *137*, 11150–11155.

(32) Abe, K.; Murakami, Y.; Tatsumi, A.; Sumida, K.; Kezuka, A.; Fukaya, T.; Kumagai, T.; Osawa, Y.; Sode, K.; Ikebukuro, K. *Chem. Commun.* **2015**, *51*, 11467–11469.

(33) Kim, M.-S.; Stybayeva, G.; Lee, J. Y.; Revzin, A.; Segal, D. J. *Nucleic Acids Res.* **2011**, *39*, e29.

(34) Stains, C. I.; Porter, J. R.; Ooi, A. T.; Segal, D. J.; Ghosh, I. J. *Am. Chem. Soc.* **2005**, *127*, 10782–10783.

(35) Osawa, Y.; Ikebukuro, K.; Motoki, H.; Matsuo, T.; Horiuchi, M.; Sode, K. *Nucleic Acids Res.* **2008**, *36*, e68.

(36) Abe, K.; Kumagai, T.; Takahashi, C.; Kezuka, A.; Murakami, Y.; Osawa, Y.; Motoki, H.; Matsuo, T.; Horiuchi, M.; Sode, K.; Igimi, S.; Ikebukuro, K. *Anal. Chem.* **2012**, *84*, 8028–8032.

(37) Das, J.; Ivanov, I.; Montermini, L.; Rak, J.; Sargent, E. H.; Kelley, S. O. *Nat. Chem.* **2015**, *7*, 569–575.

(38) Gautschi, O.; Huegli, B.; Ziegler, A.; Gugger, M.; Heighway, J.; Ratschiller, D.; Mack, P. C.; Gumerlock, P. H.; Kung, H. J.; Stahel, R. A.; Gandara, D. R.; Betticher, D. C. *Cancer Lett.* **2007**, *254*, 265–273.

(39) Wang, S.; An, T.; Wang, J.; Zhao, J.; Wang, Z.; Zhuo, M.; Bai, H.; Yang, L.; Zhang, Y.; Wang, X.; Duan, J.; Wang, Y.; Guo, Q.; Wu, M. *Clin. Cancer Res.* **2010**, *16*, 1324–1330.

(40) Soleymani, L.; Fang, Z.; Sargent, E. H.; Kelley, S. O. *Nat. Nanotechnol.* **2009**, *4*, 844–848.

(41) Soleymani, L.; Fang, Z.; Sun, X.; Yang, H.; Taft, B. J.; Sargent, E. H.; Kelley, S. O. *Angew. Chem., Int. Ed.* **2009**, *48*, 8457–8460.

(42) Das, J.; Cederquist, K. B.; Zaragoza, A. A.; Lee, P. E.; Sargent, E. H.; Kelley, S. O. *Nat. Chem.* **2012**, *4*, 642–648.

(43) Das, J.; Kelley, S. O. *Anal. Chem.* **2013**, *85*, 7333–7338.

(44) Lam, B.; Das, J.; Holmes, R. D.; Live, L.; Sage, A.; Sargent, E. H.; Kelley, S. O. *Nat. Commun.* **2013**, *4*, 1–8.

(45) Besant, J. D.; Das, J.; Sargent, E. H.; Kelley, S. O. *ACS Nano* **2013**, *7*, 8183–8189.

(46) Bin, X.; Sargent, E. H.; Kelley, S. O. *Anal. Chem.* **2010**, *82*, 5928–5931.

(47) Lapiere, M. A.; O’Keefe, M. M.; Taft, B. J.; Kelley, S. O. *Anal. Chem.* **2003**, *75*, 6327–6333.

(48) Yang, A. H.; Hsieh, K.; Patterson, A. S.; Ferguson, B. S.; Eisenstein, M.; Plaxco, K. W.; Soh, H. T. *Angew. Chem., Int. Ed.* **2014**, *53*, 3163–3167.

(49) PNAGENE (www.panagene.com). PNA Clamp KRAS Mutation Detection Kit (Ver.2), Instruction manual for product # PNAC-1002, Version 4.1 and PNA Clamp BRAF Mutation Detection Kit, Instruction manual for product # PNAC-2001, Version 4.4, 2012.

(50) Li, J.; Wang, L.; Mamon, H.; Kulke, M. H.; Berbeco, R.; Makrigiorgos, G. M. *Nat. Med.* **2008**, *14*, 579–584.

(51) Thress, K. S.; Paweletz, C. P.; Felip, E.; Cho, B. C.; Stetson, D.; Dougherty, B.; Lai, Z.; Markovets, A.; Vivancos, A.; Kuang, Y.; Ercan, D.; Matthews, S. E.; Cantarini, M.; Barrett, J. C.; Jänne, P. A.; Oxnard, G. R. *Nat. Med.* **2015**, *21*, 560–562.

(52) Baker, M. *Nat. Methods* **2012**, *9*, 541–544.

(53) Zhou, Y.; Wan, Y.; Sage, A.; Poudineh, M.; Kelley, S. O. *Langmuir* **2014**, *30*, 14322–14328.

■ NOTE ADDED AFTER ASAP PUBLICATION

This paper was published on August 19, 2016 and was partially corrected; the fully corrected version was reposted on August 31, 2016.